

# Excitations of optically driven atomic condensate in a cavity: theory of photodetection measurements

B. Öztürk,<sup>1,\*</sup> M. Bordyuh,<sup>2</sup> Ö. E. Müstecaplıoğlu,<sup>3</sup> and H. E. Türeci<sup>2,1</sup>

<sup>1</sup>*Institute for Quantum Electronics, ETH-Zürich, CH-8093 Zürich, Switzerland*

<sup>2</sup>*Department of Electrical Engineering, Princeton University, Princeton, New Jersey 08544, USA*

<sup>3</sup>*Department of Physics, Koç University, İstanbul, 34450, Turkey*

(Dated: July 18, 2011)

Recent experiments have demonstrated an open system realization of the Dicke superradiance transition in the motional degrees of freedom of an optically driven Bose-Einstein condensate in a cavity. Relevant collective excitations of this light-matter system are polaritonic in nature, allowing access to the quantum critical behavior of the Dicke model through light leaking out of the cavity. This opens the path to using photodetection based quantum optical techniques to study the dynamics and excitations of this elementary quantum critical system. We first discuss the photon flux observed at the cavity face and find that it displays a different scaling law near criticality than that obtained from the mean field theory for the equivalent closed system. Next, we study the second order correlation measurements of photons leaking out of the cavity. Finally, we discuss a modulation technique that directly captures the softening of polaritonic excitations. Our analysis takes into account the effect of the finite size of the system which may result in an effective symmetry breaking term.

PACS numbers: 03.75.Kk / 03.75.Lm / 37.10.Vz

## I. INTRODUCTION

In the study of strongly correlated systems and collective phenomena, light has traditionally assumed the role of a spectroscopic probe. Recent progress in the control of light-matter interactions through cavity QED has brought forth new systems where light and matter play equally important roles in emergent phenomena. Such hybrid light-matter systems are characterized by the existence of well-defined quasi-particles, polaritons, which are partly light partly matter-like. A crucial feature of these systems is that they are inherently out of equilibrium due to unavoidable photon-leakage, giving rise to open system analogues of certain well-studied quantum many body Hamiltonians. Such systems may for instance be formed by scaling up standard single-cavity QED systems to lattices of cavities. Recent theoretical work in Cavity QED lattices has addressed the realization of superfluid-Mott insulator transition of polaritons [1–4], fractional quantum Hall states [5], the Tonks-Girardeau gas in one-dimensional geometries [6, 7] and effective spin models [3, 8].

A different venue is to couple non-trivial states of matter to cavities, where the formation of polaritonic collective excitations may result in new emergent phenomena. One particular approach is to couple a Bose-Einstein Condensate (BEC) to a single mode of a high-finesse optical cavity. This results in tunable, long-range forces between atoms of the BEC that is mediated by the cavity field. A phase transition from a uniform BEC to a self-organized, density-modulated phase has been pre-

dicted [9] as a function of the power of the laser driving the atoms transverse to the cavity axis and experimentally observed recently [10]. A similar self-organization transition has also been observed for a thermal cloud of atoms [11]. It remains a question to distinguish the two types of transitions from each other, a matter that can be settled by studying the nature of excitations around criticality.

Here we study the excitations of the zero-temperature BEC self-organization transition, which, in the experimentally realized parameter regime, was shown to be a faithful open-system realization of the Dicke superradiance transition where spins correspond to the collective motional degrees of freedom of atoms. The transition is driven by softening of a polaritonic excitation as the critical point is approached. This provides access to the internal excitation dynamics close to criticality through photons that leak out of the cavity mirrors. Thus well-established quantum optical measurement schemes appear as specially suited to monitor the intra-cavity excitation dynamics as well as the phase diagram. We first discuss the critical behavior of photon flux measured at the cavity mirror. We then study the signature of excitations in the second order correlation functions of leaking photons, a measurement that can readily be performed using standard quantum optical schemes such as the Hanbury-Brown-Twiss setup [12]. Finally, we consider a modulation technique that directly captures the softening of the relevant polaritonic mode through the photodetection of leaking photons. Our discussion will take into account the role of the finite size of the system that is relevant for a realistic experimental setting which is shown to result in an effective symmetry-breaking term.

The paper is organized as follows. In Section II we summarize the system and the governing Hamil-

---

\*Electronic address: oztop@phys.ethz.ch

tonian together with mapping to the Dicke model. We then investigate the collective light-matter excitations in Section III. Finally we discuss three different photodetection-based measurement schemes in Section IV.

## II. MODEL OF THE SYSTEM

We consider a Bose-Einstein condensate (BEC) of length  $D$  coupled to a single mode of frequency  $\omega_c$  and decay rate  $\kappa$  of a high finesse cavity of length  $L$ , driven by a laser with frequency  $\omega_p$  from a direction perpendicular to the cavity axis [10]. We assume that  $|\Delta_c| = |\omega_p - \omega_c| \sim \kappa$  so that the cavity can be quasi-resonantly excited by the scattered pump photons from atoms. Simultaneously, the laser is red-detuned far from an internal atomic transition at  $\omega_a$ , so that  $|\Delta_a| = |\omega_p - \omega_a| \gg \gamma_a$ , where  $\gamma_a$  is the atomic linewidth. This ensures that the atoms are predominantly in their ground states during the excitation process, suppressing spontaneous emission and giving rise to an optical potential for the motional degrees of freedom of atoms  $|\hat{E}^+(\mathbf{x})|^2/\Delta_a$ . Here  $\hat{E}^+(\mathbf{x}) = g_0\varphi_c(\mathbf{x})\hat{a} + \Omega_p\varphi_p(\mathbf{x})$  is the positive rotating component of the electric field felt by an atom of the cloud at position  $\mathbf{x}$ , due to the interference of the cavity field (photon creation operator  $\hat{a}$ , atom-field coupling  $g_0$ , mode function  $\varphi_c(\mathbf{x})$ ) and a coherent laser field (with Rabi frequency  $\Omega_p$  and standing wave pattern  $\varphi_p(\mathbf{x})$ ). The Hamiltonian under these approximations is given by

$$\hat{H} = -\hbar\Delta_c\hat{a}^\dagger\hat{a} + \int d\mathbf{x} \hat{\Psi}^\dagger(\mathbf{x}) \left[ \frac{-\hbar^2}{2m}\nabla^2 + \hbar\frac{|\hat{E}^+(\mathbf{x})|^2}{\Delta_a} + V(\mathbf{x}) \right] \hat{\Psi}(\mathbf{x}). \quad (1)$$

We consider a situation where the BEC is trapped by an additional external trapping potential  $V(\mathbf{x})$  and that this is deep in the radial direction confining the cloud along the cavity axis ( $x$ ). With the additional assumption that the driving laser beam is broad, we can reduce the problem to a an effective one-dimensional problem with  $\varphi_p(\mathbf{x}) \approx \text{const.}$  (the constant to be absorbed into  $\Omega_p$ ) and  $\varphi_c(\mathbf{x}) \approx \varphi_c(x)$  [13]. We will assume that the cavity mode function is given by  $\varphi_c(x) = \frac{1}{\sqrt{L}}\sin(Gx)$  where  $G = 2\pi/\lambda_c \approx 2\pi/\lambda_p$ . The final Hamiltonian is then given by

$$\hat{H} = -\hbar\Delta_c\hat{a}^\dagger\hat{a} + \int dx \hat{\Psi}^\dagger(x) \left[ \frac{-\hbar^2}{2m}\frac{d^2}{dx^2} + V(x) + \hbar U_0 |\varphi_c(x)|^2 \hat{a}^\dagger\hat{a} + \hbar\eta\varphi_c(x)(\hat{a}^\dagger + \hat{a}) \right] \hat{\Psi}(x), \quad (2)$$

where  $U_0 = g_0^2/\Delta_a$  and  $\eta = \Omega_p g_0/\Delta_a$ . We have subtracted the energy provided by the constant potential  $\hbar\Omega_p^2/\Delta_a$ . We will neglect the contact interactions between atoms of the condensate, which is not essential for the physics discussed here.

As a function of the tunable pump power  $\eta$ , this model displays a phase transition from a non-organized phase,

a homogenous condensate, to an organized, density-modulated phase [9, 14, 15]. Below a threshold power  $\eta_c$ , the intracavity (mean) field is vanishingly small and the cloud is in the ground state of only the external trapping potential. As the critical point is crossed, the atoms self-organize into a crystalline order. This in turn results in a non-zero cavity mean-field through the scattering of the pump photons from the density-modulated atomic cloud into the cavity. In the organized phase the system chooses spontaneously between two density-modulated configurations that are shifted by half a cavity wavelength: the *even* or *odd* checkerboard configuration. This self-organization phase transition was observed experimentally for thermal atomic gas [11] and for a cloud of atomic BEC [10].

For the experimental conditions of Ref. [10], the self-organization transition can also be seen as the Dicke transition from a normal to a superradiant phase [10, 16]. We will confine ourselves to this regime but take steps to accurately model the experimental conditions. We assume a BEC considerably smaller than the cavity size, imposed by the external trapping potential  $V(x)$  and expand the field operator

$$\hat{\Psi}(x) = \sum_n \hat{c}_n \phi_n(x) \quad (3)$$

Here,  $\phi_n(x)$  is the atomic single-particle basis satisfying  $\left[ \frac{-\hbar^2}{2m}\frac{d^2}{dx^2} + V(x) \right] \phi_n(x) = \omega_n \phi_n(x)$ . We will assume  $V(x)$  to impose Neumann Boundary conditions at  $x = (L-D)/2 \pm d$  and  $x = (L+D)/2 \pm d$ , allowing for an asymmetric placement of the trap by a length  $d$  with respect to the cavity walls (we will assume  $d/D \ll 1$ ). Then,  $\phi_0(x) = 1/\sqrt{D}$  is the uniform mode of the condensate with zero momentum. In the expansion (3), we keep only one additional mode having a relatively large overlap with cavity mode  $\varphi_c(x)$ , say  $\phi_n(x)$ , which becomes the dominant contribution in the Hamiltonian of Eq. (2) when the cavity mean-field is non-zero. The corresponding wave-vector is  $k_n \approx G$ . Here it is assumed that these two modes satisfy the relation  $\hat{c}_0^\dagger \hat{c}_0 + \hat{c}_n^\dagger \hat{c}_n = N$ . Introducing the Schwinger representation for 'spins'  $\hat{J}_- = \hat{c}_0^\dagger \hat{c}_n$ ,  $\hat{J}_+ = \hat{c}_n^\dagger \hat{c}_0$  and  $\hat{J}_z = (\hat{c}_n^\dagger \hat{c}_n - \hat{c}_0^\dagger \hat{c}_0)/2$ , the final Hamiltonian can be written as

$$\begin{aligned} \hat{H}_D/\hbar &= \omega \hat{a}^\dagger \hat{a} + \omega_0 \hat{J}_z + \frac{\lambda}{\sqrt{N}} (\hat{a}^\dagger + \hat{a})(\hat{J}_+ + \hat{J}_-) \\ &\quad + \frac{\lambda'}{\sqrt{N}} (\hat{a}^\dagger + \hat{a}) \left( \frac{N}{2} - \hat{J}_z \right) \end{aligned} \quad (4)$$

where  $\omega = -\Delta_c + (NU_0/D) \int dx |\varphi_c(x)|^2$ ,  $\omega_0 = \omega_R = \hbar G^2/2m$ ,  $\lambda = (\sqrt{N/D})\eta \int dx \varphi_c(x)\phi_n(x)$  and  $\lambda' = (\sqrt{N/D})\eta \int dx \varphi_c(x)\phi_0(x)$ . In all of our calculations here, the limits of the overlap integrals are those of the atomic trap since  $\phi_n(x) = 0$  outside. Since we are interested in the critical behavior, an additional dispersive shift term [10] which is negligible near critical point is dropped in Eq. (4).

For  $\lambda' = 0$ , Eq. 4 is the well-known single-mode Dicke Hamiltonian. In the thermodynamic limit of  $N \gg 1$ , the Dicke Hamiltonian (4) exhibits a quantum phase transition at a critical coupling strength  $\lambda_c = (1/2)\sqrt{\omega\omega_0}$  from a normal phase with  $\langle a \rangle = \langle J_- \rangle = 0$  to a superradiant phase [17–24] with  $\langle a \rangle \neq 0$ ,  $\langle J_- \rangle \neq 0$ . The parity symmetry of the Dicke Hamiltonian (4) under  $(\hat{a} \rightarrow -\hat{a}, \hat{J}_- \rightarrow -\hat{J}_-)$  gives rise to two distinct degenerate superradiant phases that break the parity symmetry of the Hamiltonian.

We observe that a non-zero  $\lambda'$  acts as a symmetry-breaking bias field where the sign of  $\lambda'$  determines which state is chosen in the superradiant phase. If a trap is not positioned perfectly symmetrically with respect to the middle of the cavity,  $\lambda' \neq 0$ . This was observed in recent experiments studying the process of symmetry breaking in real time through an interferometric heterodyne detection scheme [25].

Finally, cavity losses at a rate  $\kappa$  can be included through a Lindblad master equation approach [26]. Note that this leads to an open-system analogue of the Dicke superradiance transition, which, most significantly results in a shift of the critical point to  $\lambda_c = (1/2)\sqrt{(\omega_0/\omega)(\kappa^2 + \omega^2)}$ . A second important consequence is that the excitation spectrum and the dynamics becomes dissipative.

Introducing mean fields  $\alpha = \langle \hat{a} \rangle$ ,  $\beta = \langle \hat{J}_- \rangle$  and  $w = \langle \hat{J}_z \rangle$  in the Heisenberg equations of motion for the system Hamiltonian (4), one gets

$$\dot{\alpha} = -(\kappa + i\omega)\alpha - i\frac{\lambda}{\sqrt{N}}(\beta + \beta^*) - i\frac{\lambda'}{\sqrt{N}}\left(\frac{N}{2} - w\right), \quad (5a)$$

$$\dot{\beta} = -i\omega_0\beta + 2i\frac{\lambda}{\sqrt{N}}(\alpha + \alpha^*)w + i\frac{\lambda'}{\sqrt{N}}\beta(\alpha + \alpha^*), \quad (5b)$$

$$\dot{w} = i\frac{\lambda}{\sqrt{N}}(\alpha + \alpha^*)(\beta - \beta^*), \quad (5c)$$

These equations have to be solved with the constraint that pseudo angular momentum  $|\beta|^2 + w^2 = N^2/4$  is conserved. Analytical solutions can be found for this set of nonlinear equations in the steady-state when  $\lambda' = 0$  [26]. In that case, the steady state solution displays a bifurcation point at  $\lambda = \lambda_c$ . While  $\alpha_{ss} = \beta_{ss} = 0$  is the trivial solution for all values of  $\lambda$ , it's only stable for  $\lambda < \lambda_c$ . For  $\lambda > \lambda_c$ , this solution becomes unstable and two new set of stable solutions appear given by [26]

$$\alpha_{ss} = \pm\sqrt{N}\frac{\lambda}{\omega - i\kappa}\sqrt{1 - \frac{\lambda_c^4}{\lambda^4}}, \quad (6a)$$

$$\beta_{ss} = \mp\frac{N}{2}\sqrt{1 - \frac{\lambda_c^4}{\lambda^4}}, \quad (6b)$$

The behavior of these solutions for  $\alpha_{ss}$  are shown in Fig. 1(a). For  $\lambda' \neq 0$ , the bifurcation point (and the

threshold) disappears and the stable solution becomes nonzero for all  $\lambda > 0$  values (Fig. 1(c,d)). We do not plot  $\beta$ , it displays a similar behavior to  $\alpha$ , with its sign opposite to that of  $\alpha$ . Here, we should note that the spatial structure of the self-organized state, as shown in Fig. 1(b), depends on the sign of  $\lambda'$ .

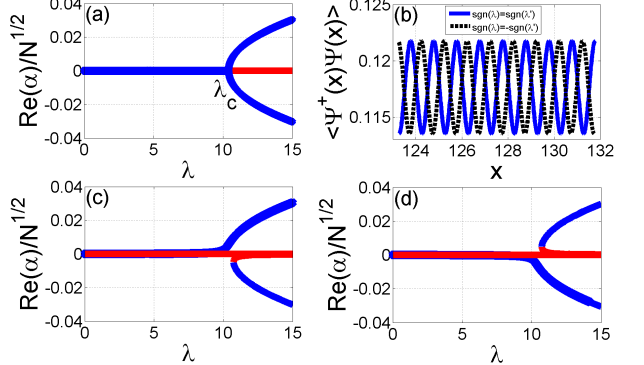


FIG. 1: (a) The real part of  $\alpha$  for  $\lambda' = 0$ . Below threshold the stable solution is  $\alpha = 0$  and above threshold there are two stable solutions with a phase difference  $\pi$ . (b) The steady state atomic density profiles for  $\lambda' < 0$  and  $\lambda' > 0$  with  $\lambda = 9$  and  $\lambda'/\lambda \approx \pm 120$ . (c) Dependence of  $\alpha$  on the coupling parameter for the trap displaced to the right, which corresponds to  $sgn(\lambda) = sgn(\lambda')$ . (d) Same as (c) except that the displacement of the trap is to the left so that  $sgn(\lambda) = -sgn(\lambda')$ . In (a), (c) and (d) blue (red) lines represent stable (unstable) solutions. For all of the calculations, we use the parameters  $\omega = 300$ ,  $\kappa = 200$ ,  $\omega_0 = 1$  and for these choice of parameters  $\lambda_c \approx 10.41$ .

### III. POLARITONIC EXCITATIONS

In this section, we investigate the collective light-matter excitations of the system that play an crucial role in the course of the underlying phase transition. To this end, we employ Holstein-Primakoff transformation to express the atomic spin operators in terms of bosonic mode operators  $\hat{b}$  and  $\hat{b}^\dagger$  such as  $\hat{J}_+ = \hat{b}^\dagger\sqrt{N - \hat{b}^\dagger\hat{b}}$ ,  $\hat{J}_- = \hat{J}_+^\dagger$  and  $\hat{J}_z = \hat{b}^\dagger\hat{b} - N/2$  [24, 26]. Substituting these expressions into the Dicke Hamiltonian (4) and expanding in the limit  $N \gg 1$ , we get the Hamiltonian governing the fluctuations around the steady state semiclassical solutions  $\alpha_{ss}$  and  $\beta_{ss}$

$$\hat{H}_{HP}/\hbar = \omega\hat{c}^\dagger\hat{c} + \omega'_0\hat{d}^\dagger\hat{d} + g_1(\hat{d}^\dagger + \hat{d})^2 + g_2(\hat{c}^\dagger + \hat{c})(\hat{d}^\dagger + \hat{d}) \quad (7)$$

where  $\hat{c}$  and  $\hat{d}$  are the photonic and atomic fluctuation operators respectively,  $\hat{a} = \alpha_{ss} + \hat{c}$  and  $\hat{b} = \beta_{ss}/\sqrt{N} + \hat{d}$ , and

$$\omega'_0 = \omega_0 - 2\lambda\frac{\tilde{\beta}_{ss}}{\sqrt{1 - \tilde{\beta}_{ss}^2}}\text{Re}(\tilde{\alpha}_{ss}), \quad (8a)$$

$$g_1 = -\lambda \frac{\tilde{\beta}_{ss}(2 - \tilde{\beta}_{ss}^2)}{2(1 - \tilde{\beta}_{ss}^2)^{3/2}} \text{Re}(\tilde{\alpha}_{ss}), \quad (8b)$$

$$g_2 = \lambda \frac{1 - 2\tilde{\beta}_{ss}^2}{\sqrt{1 - \tilde{\beta}_{ss}^2}} - \lambda' \tilde{\beta}_{ss}. \quad (8c)$$

Here we introduced the scaled variables  $\tilde{\alpha}_{ss} = \alpha_{ss}/\sqrt{N}$ ,  $\tilde{\beta}_{ss} = \beta_{ss}/N$ . One should note that the steady-state values  $\alpha_{ss}$  and  $\beta_{ss}$  are  $\lambda'$ -dependent. The quadratic Hamiltonian above leads to linear equations of motion  $\dot{\mathbf{h}} = \mathbf{M}\mathbf{h}$  for fluctuations  $\mathbf{h} = (\langle \hat{c} \rangle, \langle \hat{c}^\dagger \rangle, \langle \hat{d} \rangle, \langle \hat{d}^\dagger \rangle)$ . This was done in the resonant case for  $\omega = \omega_0$  and  $\lambda' = 0$  in Ref. [26]. Here we are interested in the dispersive cavity regime of the self-organization problem [10, 16] for which  $\omega_0^2 \ll \omega^2 + \kappa^2$ . In that regime the real and imaginary parts of the lowest excitation eigenvalues are shown in Fig. 2 with  $\lambda' = 0$ . The real parts of the remaining two eigenvalues are very large compared to those shown in the figure due to the dispersive nature of the cavity and are not shown. By employing perturbation theory for the small parameter  $\varepsilon = \omega_0^2/(\omega^2 + \kappa^2)$ , the real and imaginary parts of the polaritonic eigenvalue up to  $O(\varepsilon^2)$  are calculated as

$$\omega_{ex} = \omega_0 \sqrt{1 - \frac{\lambda^2}{\lambda_c^2}} \left( 1 + \frac{1}{2} \frac{\omega_0^2}{\omega^2 + \kappa^2} \frac{\lambda^2}{\lambda_c^2} \right) - i \frac{\kappa \omega_0^2}{\omega^2 + \kappa^2} \frac{\lambda^2}{\lambda_c^2}. \quad (9)$$

We observe that the energy gap monotonously decreases and the lowest energy mode “softens” as we approach the critical point from below. Note that this is the atomic excitation at  $\lambda = 0$  which gradually acquires a photonic component as we approach the critical point, therefore we refer to this collective excitation as polaritonic. This is also the reason why the imaginary part of this excitation becomes larger, as in Fig. 2, as the critical point is approached. We note however that there is a very narrow regime around  $\lambda_c$  in Fig. 2 where the excitation energy  $\text{Re}(\omega_{ex})$  is zero and the damping  $\text{Im}(\omega_{ex})$  decreases towards the critical point. In this regime of critical slowing down fluctuations are overdamped. This regime is characterized by two values  $\lambda_1 < \lambda_c$  and  $\lambda_2 > \lambda_c$  below and above threshold respectively. For the dispersive cavity case, these two values can be approximated by

$$\lambda_1 \simeq \lambda_c \left[ 1 - \frac{\kappa^2 \omega_0^2}{(\omega^2 + \kappa^2)^2} \right], \quad \lambda_2 \simeq \lambda_c \left[ 1 + \frac{1}{2} \frac{\kappa^2 \omega_0^2}{(\omega^2 + \kappa^2)^2} \right]. \quad (10)$$

The behavior of  $\omega_{ex}$  in this range is drastically different from Eq. (9) and is given to order  $(1 - \lambda^2/\lambda_c^2)$  by

$$\omega_{ex} \approx -i \frac{(\omega^2 + \kappa^2)}{2\kappa} \left( 1 - \frac{\lambda^2}{\lambda_c^2} \right) \quad (11)$$

below threshold.

The existence of this collective soft mode is significant for two reasons. Firstly, near the critical point this

mode provides a fluctuation channel that drives the non-equilibrium phase transition. Secondly, due to the increasing light-like content of this channel, we get a first-hand look into the fluctuations around the critical point by monitoring photons that leak out of the cavity.

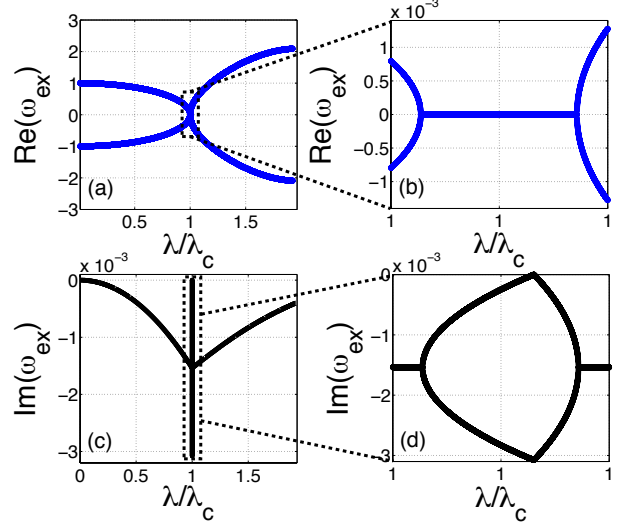


FIG. 2: The real and imaginary parts of the eigenfrequencies of *polaritonic* excitations. Parameters are the same ones used in Fig. 1. The figures on the right column show the indicated magnified views of real and imaginary parts around  $\lambda = \lambda_c$ .

#### IV. PHOTODETECTION MEASUREMENTS OF CAVITY PHOTONS

Photon flux that leaks out of the cavity below the threshold is very low. Therefore, photodetection measurements appear to be most useful for characterizing critical fluctuations. We consider below two measurement schemes, direct photon counting and second order photon correlations that can be implemented with standardly available photon counters. In section Section IV C, we discuss a modulation scheme which provides a direct access to the softening behavior of the polaritonic mode.

To this end, we make use of the standard input-output formalism [26, 27], introducing the photonic input and output operators  $\hat{a}_{in}, \hat{a}_{out}$ , that couple to the intra-cavity fluctuation operators  $\hat{c}$  and  $\hat{d}$  in the following manner:

$$\dot{\hat{c}} = -(i\omega + \kappa)\hat{c} - ig_2(\hat{d} + \hat{d}^\dagger) + \sqrt{2\kappa}\hat{a}_{in}, \quad (12a)$$

$$\dot{\hat{d}} = -i\omega'_0\hat{d} - 2ig_2(\hat{d} + \hat{d}^\dagger) - ig_2(\hat{c} + \hat{c}^\dagger), \quad (12b)$$

with  $\hat{a}_{in}$  being operator for the quantum noise incident on the semi-transparent cavity wall satisfying the commutations relation  $[\hat{a}_{in}(t), \hat{a}_{in}^\dagger(t')] = \delta(t-t')$ . For vacuum input, the relation  $\langle \hat{a}_{in}^\dagger(t)\hat{a}_{in}(t') \rangle = \langle \hat{a}_{in}(t)\hat{a}_{in}(t') \rangle = 0$

holds. The cavity output can then be expressed as  $\hat{a}_{out}(t) = \sqrt{2\kappa}[\hat{c}(t) + \alpha_{ss}] - \hat{a}_{in}(t)$ .

### A. Photon counting

The photon flux measured outside the cavity can be expressed as  $I_{ss} = \langle \hat{a}_{out}^\dagger(t)\hat{a}_{out}(t) \rangle = 2\kappa\langle \hat{c}^\dagger(t)\hat{c}(t) \rangle$ . The photon flux was numerically found to diverge at the critical point [16, 26] but the precise form of scaling law was not elaborated on. We find that the intra-cavity photon number is given by

$$\langle \hat{c}^\dagger(t)\hat{c}(t) \rangle_{ss} = \frac{\lambda^2}{8\lambda_c^2 [1 - (\lambda/\lambda_c)^2]} \quad (13)$$

clearly displaying non-equilibrium mean field critical scaling with an exponent  $\gamma_{neq} = 1$ . We note that this scaling is drastically different than that of the equilibrium, ground state expectation value of the intra-cavity photon number:

$$\langle \hat{c}^\dagger(t)\hat{c}(t) \rangle_{gs} \approx \frac{\lambda^2}{\omega^2 \sqrt{1 - (\lambda/\lambda_c)^2}} \quad (14)$$

obtained through perturbation theory in  $\varepsilon = \omega_0^2/(\omega^2 + \kappa^2)$ . The latter displays an exponent  $\gamma_{eq} = 1/2$  as expected from standard equilibrium mean-field systems. The reason behind this is the depletion of the ground state (for  $T = 0$ ) through coupling to the photonic environment. This possibility was hinted on in Ref [16], but the authors only calculated the rate of depletion in the short-time limit i.e. in the transient regime. We find here that the depletion settles at a steady state, giving rise to an entirely different scaling law for incoherent fluctuations of intracavity photons as critical point is approached. Note that the two expressions do not even agree for  $\kappa \rightarrow 0$  that enters the non-equilibrium expression through the form of  $\lambda_c$ . However, it should be pointed out that the limit  $\kappa \rightarrow 0$  is a singular limit and has to be considered with care. The steady-state regime where this expression holds is shifted to  $t \rightarrow \infty$  as  $\kappa \rightarrow 0$ . This time scale can be calculated from the imaginary part of the polaritonic excitation branch and is found to scale as  $|\text{Im}(\omega_{ex})|^{-1} \approx \omega^3/(4\omega_0\lambda^2\kappa)$  according to Eq. (9). For  $\kappa = 0$ , a steady state will never be reached unless the system starts out in the ground state. What remains to be seen is whether open quantum systems may be forming an entirely new universality class.

### B. Second order correlations of photons

The second order correlation function of leaking photons  $g^{(2)}(t, \tau)$  is given by

$$g^{(2)}(t, \tau) = \frac{\langle \hat{a}_{out}^\dagger(t)\hat{a}_{out}^\dagger(t+\tau)\hat{a}_{out}(t+\tau)\hat{a}_{out}(t) \rangle}{\langle \hat{a}_{out}^\dagger(t)\hat{a}_{out}(t) \rangle^2}. \quad (15)$$

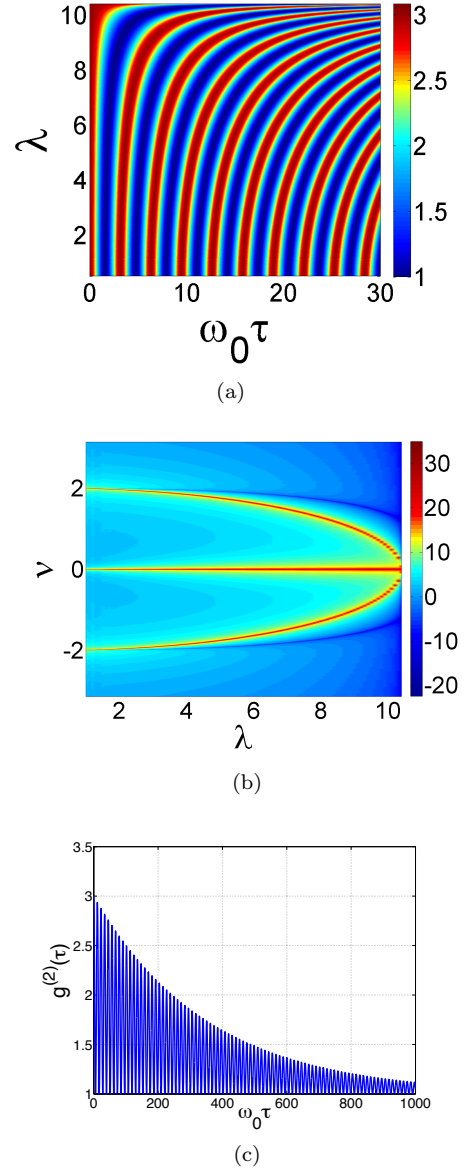


FIG. 3: (a) False color plot of the dependence of the steady-state second order correlation function  $g_{ss}^{(2)}(\tau)$  on  $\lambda$ . We observe that the period of the oscillations increase with increasing  $\lambda$ . Note that  $g_{ss}^{(2)}(\tau = 0, \lambda) = 3$ . (b) The logarithm of the Fourier transform of  $g_{ss}^{(2)}$  (color code) is plotted as a function of frequency  $\nu$  and the coupling parameter  $\lambda$ . The two peaks other than the one at  $\nu = 0$  appear at  $\nu = \pm 2\omega_0\sqrt{1 - (\lambda^2/\lambda_c^2)}$ . In both figures  $\lambda' = 0$ . The system parameters are same as in Fig. 2. (c) The long-time behavior of  $g_{ss}^{(2)}(\tau)$  displaying an exponential decay of the envelope of its oscillations.

By using the input-output relations and the vacuum nature of the input noise, in the steady-state the expres-

sion in Eq. (15) can be simplified to

$$g^{(2)}(t, \tau) = 1 + |g^{(1)}(t, \tau)|^2 + \frac{|\langle \hat{c}(t + \tau)\hat{c}(t) \rangle + \alpha_{ss}^2|^2 - 2|\alpha_{ss}|^4}{(\langle \hat{c}^\dagger(t)\hat{c}(t) \rangle + |\alpha_{ss}|^2)^2}, \quad (16)$$

where  $g^{(1)}(t, \tau) = \langle \hat{c}^\dagger(t + \tau)\hat{c}(t) \rangle / \langle \hat{c}^\dagger(t)\hat{c}(t) \rangle$  is the first order correlation function. This steady-state form can be calculated by solving the Eqs. (12) together with their adjoints in Fourier space. Some of the results for  $\lambda' = 0$  are shown in Fig. 3 for different  $\lambda < \lambda_c$  values. It can be seen that  $g_{ss}^{(2)}(\tau)$  displays underdamped oscillations with the oscillation period progressively increasing as critical point is approached. A Fourier analysis of the oscillations in  $g_{ss}^{(2)}(\tau)$  as a function of  $\lambda$  is shown in Fig. 3(b). We observe that the position of the peaks  $\nu_{peak}$  follow very closely the excitation frequency of the softening polaritonic mode given by Eq. (9); indeed it can be shown that  $\nu_{peak}(\lambda) \approx 2\text{Re}[\omega_{ex}(\lambda)]$ . The width of the peaks, not resolvable for parameters chosen here, is proportional to  $\text{Im}[\omega_{ex}(\lambda)]$ . One can furthermore show that  $g_{ss}^{(2)}(0) = 3$  as a consequence of the identity  $|\langle \hat{c}^\dagger(t)\hat{c}(t) \rangle_{ss}| = |\langle \hat{c}(t)\hat{c}(t) \rangle_{ss}|$ , indicating that the evolution of the system is into a two-mode squeezed state in the steady state. The above analysis provides a unique window into the nature of fluctuations close to the critical point.

We next calculate  $g_{ss}^{(2)}(\tau)$  for nonzero values of  $\lambda'$ . Here, the second order correlation function displays a beating pattern in time as seen in Fig. 4. This is the consequence of a non-vanishing mean-field  $\alpha_{ss}$  extending all the way below the threshold, providing a non-zero dc component  $\alpha_{ss}$  in Eq. (16). Thus such a distinct beating pattern is a signature of the interference of a non-zero coherent cavity field and incoherent photons.

### C. Modulation Spectroscopy

In this subsection, we analyze a modulation technique that provides an alternative access window into critical fluctuations. This technique relies on parametric resonances of the cavity-BEC system and is similar to modulation techniques applied to the analysis of ultracold gases [28–31].

While various parameters of the system may be modulated, we choose one that appears to be experimentally most straightforward: modulation of the transverse pump power. We assume a periodic modulation of the pump Rabi frequency,  $\eta(t) = \eta[1 + \epsilon \cos(\nu t)]$  where  $\nu$  is the modulation frequency and  $\epsilon \ll 1$ , resulting in the modulation of the coupling parameter  $\lambda(t) = \lambda[1 + \epsilon \cos(\nu t)]$  in the Dicke model, Eq. (4). Here we analyze the case  $\lambda' = 0$ . The analysis below can straightforwardly be extended to non-zero  $\lambda'$ .

We assume  $\kappa \gg \omega_0$ , so that the cavity field dynamics adiabatically follows the atomic dynamics and the photon

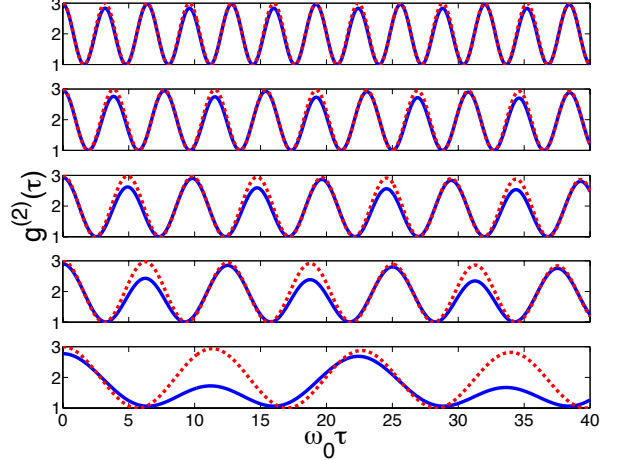


FIG. 4:  $g_{ss}^{(2)}(\tau)$  for  $\lambda' = \lambda/360$  is represented by blue solid lines and for the case  $\lambda' = 0$  (i.e.  $\alpha_{ss} = 0$ ) by dashed red lines. From top to bottom,  $\lambda = 2, 6, 8, 9, 10$ . The asymmetry in adjacent peaks is due to the presence of nonzero mean-field  $\alpha_{ss}$ . The system parameters are as in Fig. 2.

field  $\alpha$  can be eliminated adiabatically. This results in the following equation for the atomic variable  $\beta$ :

$$\dot{\beta} = -i\omega_0\beta + 4i\lambda^2(t) \frac{\omega}{\omega^2 + \kappa^2} \left( \frac{1}{4} - |\beta|^2 \right)^{1/2} (\beta + \beta^*), \quad (17)$$

where we used the stable solution for  $w$  which is negative. Writing  $\beta = \beta_{ss} + \delta\beta(t)$ , assuming small fluctuations around the steady state, we obtain the following equation for  $u(t) \equiv \delta\beta(t) + \delta\beta^*(t)$

$$\frac{\partial^2}{\partial \tilde{t}^2} u + [A - 2\tilde{\epsilon} \cos(\frac{\nu}{\omega_0}\tilde{t})] u = 0, \quad (18)$$

This is the well known Mathieu equation with  $A = 1 - (\lambda/\lambda_c)^2$ ,  $\tilde{\epsilon} = (\lambda/\lambda_c)^2\epsilon$  and  $\tilde{t} = \omega_0 t$ . According to the Floquet theorem, the solutions to this equation have the form  $u(\tilde{t}) = \exp(i\mu\tilde{t})\phi(\tilde{t})$  where  $\phi(\tilde{t})$  is a periodic function with period  $2\pi\omega_0/\nu$  [32]. One can readily see that the solutions  $u(\tilde{t})$  are unstable if  $\text{Re}(\mu) > 0$ . We performed a perturbative stability analysis to determine the stability boundary for the solutions [32]. We find that the instability appears when the condition

$$\nu = 2\omega_0 \sqrt{1 - \left( \frac{\lambda}{\lambda_c} \right)^2}, \quad (19)$$

is fulfilled. This leading order expression is precisely twice the excitation frequency of Eq. (9). Finally, we check our result by solving the system of coupled nonlinear equations (5a) and (5b) in real time. In Fig. 5, we plot for each modulation frequency  $\nu$  the maximum number of photons after the oscillation has stabilized, starting with very small initial  $(\alpha, \beta)$ . Thus when the frequency of modulation is chosen correctly, there will be

a substantial photon flux at the cavity face, even below threshold. We should also note that there is a broadening in resonance modulation frequencies as the critical point is approached (see Fig. 5), and this is consistent with the behavior of the imaginary part of the eigenmode in Fig. 2.

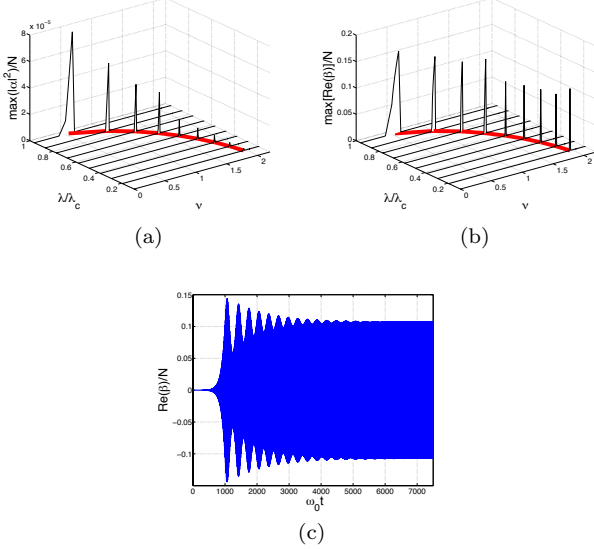


FIG. 5: (a) The maximum number of photons  $|\alpha|^2$  and (b) the maximum value for  $\text{Re}(\beta)$ , as functions of the coupling strength  $\lambda$  and the modulation frequency  $\nu$ . The peaks occur at  $\nu = 2\text{Re}(\omega_{ex})$  where  $\omega_{ex}$  is given by Eq. (9). In both figures the red curves show the instability condition Eq. (19). (c) The oscillations of  $\text{Re}(\beta)/N$  in time are shown for  $\lambda = 0.8\lambda_c$  where the modulation frequency is chosen to be equal to resonance frequency given by  $\nu = 1.2\omega_0$ . For all figures here,  $\epsilon = 1/50$  and system parameters are same as in Fig. 2.

## V. CONCLUSION

In this work, we discussed the excitations of an optically driven atomic condensate coupled to a single mode of a high-finesse cavity that displays a self-organization transition as a function of the driving strength. Taking into account the finite-size of the system, we showed

that the coupled BEC-cavity system can be mapped into an open-system realization of the Dicke model with a symmetry-breaking field.

The zero-field phase transition is driven by softening of polaritonic excitations, which provides access to the internal dynamics of the coupled system close to the criticality. We discuss a number of photodetection-based techniques for the photons that leak out of the cavity mirrors and relate it to intra-cavity critical dynamics.

We find that the intra-cavity photon number, which can be measured by a photodetector outside the cavity, displays a different scaling law for the open system than the closed system with perfectly reflecting mirrors. In the latter case, the dynamics conserves total excitation number and the photon number is calculated in the ground state.

We next discussed the second order correlation function for photons  $g_{ss}^{(2)}(\tau)$  in the steady state, via coincidence measurement of photons leaking out of the cavity walls. We show that  $g_{ss}^{(2)}(\tau)$  displays damped oscillations with a period that increases progressively as the critical point is approached, signalling the critical slowing down of the coupled intra-cavity dynamics. We relate the spectral content of the time-series of  $g_{ss}^{(2)}(\tau)$  to the complex frequency of the softening polaritonic mode. We also show that trap misalignment can lead to a background coherent cavity field and that its signature is a characteristic beating pattern in  $g_{ss}^{(2)}(\tau)$ .

Finally, we discussed a modulation scheme that directly captures the softening of the polaritonic mode. This is done by introducing a parametric instability in the system through the periodic modulation of the drive Rabi frequency in time. We show that modulation at twice the polaritonic mode frequency results in a measurable photon flux outside the cavity below the threshold.

## Acknowledgments

The authors thank K. Baumann, F. Brennecke, R. Mottl, T. Esslinger, D. A. Huse, A. Pal, S. Schmidt, M. Schiro, S. Shinozaki for stimulating discussions. H.E.T. acknowledges support from Swiss NSF under Grant No. PP00P2-123519/1. Ö.E.M. acknowledges support by TUBITAK for the Project No. 109T267.

- 
- [1] M. J. Hartmann, F. G. S. L. Brandão, and M. B. Plenio, *Nature Phys.* **2**, 849 (2006).  
[2] A. D. Greentree, C. Tahan, J. H. Cole, and L. C. L. Hollenberg, *Nature Phys.* **2**, 856 (2006).  
[3] D. G. Angelakis, M. F. Santos, and S. Bose, *Phys. Rev. A* **76**, 031805(R) (2007).  
[4] A. Tomadin, V. Giovannetti, R. Fazio, D. Gerace, I. Carusotto, H. E. Türeci, and A. Imamoglu, *Phys. Rev. A* **81**, 061801(R) (2010).  
[5] J. Cho, D. G. Angelakis, and S. Bose, *Phys. Rev. Lett.* **101**, 246809 (2008).  
[6] D. E. Chang, V. Gritsev, G. Morigi, V. Vuletic, M. D. Lukin, and E. A. Demler, *Nature Phys.* **4**, 884 (2008).  
[7] I. Carusotto, D. Gerace, H. E. Türeci, S. D. Liberato, C. Ciuti, and A. Imamoglu, *Phys. Rev. Lett.* **103**, 033601 (2009).  
[8] M. J. Hartmann, F. G. S. L. Brandão, and M. B. Plenio, *Phys. Rev. Lett.* **99**, 160501 (2007).

- [9] P. Domokos and H. Ritsch, Phys. Rev. Lett. **89**, 253003 (2002).
- [10] K. Baumann, C. Guerlin, F. Brennecke, and T. Esslinger, Nature **464**, 1301 (2010).
- [11] A. T. Black, H. W. Chan, and V. Vuletić, Phys. Rev. Lett. **91**, 203001 (2003).
- [12] R. H. Brown and R. Q. Twiss, Nature **177**, 27 (1956).
- [13] C. Maschler, I. B. Mekhov, and H. Ritsch, Eur. Phys. J. D **46**, 545 (2008).
- [14] J. K. Asbóth, P. Domokos, H. Ritsch, and A. Vukics, Phys. Rev. A **72**, 053417 (2005).
- [15] D. Nagy, G. Szirmai, and P. Domokos, Eur. Phys. Jour. D **48**, 127 (2008).
- [16] D. Nagy, G. Kónya, G. Szirmai, and P. Domokos, Phys. Rev. Lett. **104**, 130401 (2010).
- [17] K. Hepp and E. H. Lieb, Ann. Phys. (N.Y.) **76**, 360 (1973).
- [18] K. Hepp and E. H. Lieb, Phys. Rev. A **8**, 2517 (1973).
- [19] Y. K. Wang and F. T. Hioe, Phys. Rev. A **7**, 831 (1973).
- [20] F. T. Hioe, Phys. Rev. A **8**, 1440 (1973).
- [21] H. J. Carmichael, C. W. Gardiner, and D. F. Walls, Phys. Lett. **46A**, 47 (1973).
- [22] G. C. Duncan, Phys. Rev. A **9**, 418 (1974).
- [23] C. Emary and T. Brandes, Phys. Rev. Lett. **90**, 044101 (2003).
- [24] C. Emary and T. Brandes, Phys. Rev. E **67**, 066203 (2003).
- [25] K. Baumann, R. Mottl, F. Brennecke, and T. Esslinger, arXiv:1105.0426v1 (2011).
- [26] F. Dimer, B. Estienne, A. S. Parkins, and H. J. Carmichael, Phys. Rev. A **75**, 013804 (2007).
- [27] D. F. Walls and G. J. Milburn, *Quantum optics* (Springer-Verlag, Berlin Heidelberg, 2008).
- [28] C. Tozzo, M. Kramer, and F. Dalfovo, Phys. Rev. A **72**, 023613 (2005).
- [29] T. Stöferle, H. Moritz, C. Schori, M. Köhl, and T. Esslinger, Phys. Rev. Lett. **92**, 130403 (2004).
- [30] C. Schori, T. Stöferle, H. Moritz, M. Köhl, and T. Esslinger, Phys. Rev. Lett. **93**, 240402 (2004).
- [31] M. Köhl, H. Moritz, T. Stöferle, C. Schori, and T. Esslinger, J. Low. Temp. Phys. **138**, 635 (2005).
- [32] C. M. Bender and S. A. Orszag, *Advanced Mathematical Methods for Scientists and Engineers* (Springer-Verlag, New York, 1999).